mathematics

MDPI

Article

Global Dynamics and Optimal Control of a Fractional-Order SIV Epidemic Model with Nonmonotonic Occurrence Rate

Juhui Yan †, Wanqin Wu *,†, Qing Miao *,† and Xuewen Tan †

School of Mathematics and Computer Science, Yunnan Minzu University, Yuehua Street No. 2929, Chenggong District, Kunming 650500, China; 23213037570003@ymu.edu.cn (J.Y.); tanxw0910@ymu.edu.cn (X.T.)
* Correspondence: 041379@ymu.edu.cn (W.W.); 041087@ymu.edu.cn (Q.M.)
† These authors contributed equally to this work.

Abstract: This paper performs a detailed analysis and explores optimal control strategies for a fractional-order SIV epidemic model, incorporating a nonmonotonic incidence rate. In this paper, the population of vaccinated individuals is included in the disease dynamics model. After proving the non-negative boundedness of the fractional-order SIV model, we focus on analyzing the equilibrium point characteristics of the model, delving into its existence, uniqueness, and stability analysis. In addition, our research includes formulating optimal control strategies specifically aimed at minimizing the number of infections while keeping costs as low as possible. To validate the theoretical findings and uncover the practical efficacy and prospects of control measures in mitigating epidemic spread, numerical simulations are performed.

Keywords: fractional-order SIV model; fractional optimal control; global stability; nonmonotonic occurrence rate

MSC: 37N25; 49J99; 65P99

Citation: Yan, J.; Wu, W.; Miao, Q.; Tan, X. Global Dynamics and Optimal Control of a Fractional-Order SIV Epidemic Model with Nonmonotonic Occurrence Rate. *Mathematics* **2024**, *12*, 2735. https://doi.org/10.3390/math12172735

Academic Editors: Yiming Chen, Aimin Yang, Jiaquan Xie and Yanqiao Wei

Received: 3 August 2024
Revised: 27 August 2024
Accepted: 29 August 2024
Published: 1 September 2024

1. Introduction

Throughout the early 21st century, the globe has been beset by recurrent outbreaks of novel infectious diseases, which constitute a formidable hazard to human well-being and the very essence of life's safety [1]. Instances include the severe acute respiratory syndrome (SARS) epidemic in 2003 [2,3] and the recent novel coronavirus pneumonia (COVID-19) outbreak towards the conclusion of 2019 [4–6], both of which underscore the ongoing global challenge posed by infectious diseases. The outbreak and spread of these epidemics have brought tremendous challenges to the global public health system and prompted researchers to pay more attention to the study of infectious disease dynamics. Among them, the epidemic research method based on mathematical models has received widespread attention because it is capable of quantitatively portraying the transmission dynamics of diseases, enabling forecasts regarding the evolution and progression of epidemic outbreaks [7].

Vaccination is crucial for eliminating infectious diseases, such as hepatitis B, measles, smallpox, poliomyelitis, and so on [8,9]. Since the pioneering work on smallpox of Edward Jenner (a doctor who worked in the UK and noticed that people infected with cowpox rarely contracted smallpox) [10], the practice of safeguarding individuals against infections via vaccination has evolved into a standard and routine procedure. However, achieving full vaccination coverage among all susceptible individuals within a given community remains a formidable challenge, particularly in nations where accessibility to such vaccines is hindered [11]. Certain clinical findings suggest that vaccines may confer only a temporary degree of protection against certain diseases. Hence, when a vaccine's effectiveness diminishes within a vaccinated individual's system, they once again become vulnerable

to contracting the disease [12]. Consequently, identifying the optimal level of vaccination needed to eliminate a disease becomes paramount.

The incidence rate of a disease, which signifies the quantity of fresh cases arising within a specified time frame, holds significant weight in the realm of mathematical epidemiology research. Conventional epidemic models often utilize standard and bilinear incidence rates, like βSI (with β denoting the transmission rate) [7] and $\frac{\beta SI}{N}$ (where N represents the total population) [5], to depict the occurrence of new infections within a population. However, it is increasingly acknowledged that the utilization of linear incidence rates may fall short in precisely capturing the intricate progression patterns of infectious diseases within a population. In order to overcome this limitation, scientists and investigators have explored nonlinear incidence rates as a potential solution. For example, in their research of cholera outbreaks in Paris, Capasso and Serio [13] first proposed a nonlinear incidence rate with saturation effects. They further introduced the concept of saturated incidence rate into infectious disease models, specifically in the form of $g(I)S$, where g is a non-negative function with $g(0) = 0$ that ultimately tends to a saturation level. As research on infectious disease models has progressed, the form of saturated incidence rates has also become more complex. W. Liu et al. [14] proposed a general incidence rate in the form of $\frac{\beta SI^a}{1+\lambda I^b}$, where a and b are positive constants and λ is a positive parameter, used to consider the influence of changes in the behavior of susceptible individuals. Furthermore, λ determines the magnitude of psychological or inhibitory effects, while $1 + \lambda I^b$ represents how behavioral changes slow disease spread by reducing effective transmission as infected cases I increase, or what is known as the crowding effect of I.

Researchers have constructed and analyzed various mathematical models to investigate the influence of vaccines on the transmission of infectious diseases. Ref. [15] explored the SIS model in the context of partially effective vaccination, assuming that the vaccination strategy is primarily targeted at susceptible individuals while the total population size remains constant and that the spread of disease adheres to a standard incidence rate. In contrast, ref. [16] considered the same model in an environment where the overall population size is subject to change and assumed that the vaccine is fully effective for all susceptible individuals as well as newly arrived members of the population. Meanwhile, refs. [17,18], respectively, studied similar models with differing assumptions regarding incidence rates and population sizes. Ref. [19] presented a discrete-time SIS model that includes a vaccination scheme, with disease transmission occurring at a saturated incidence rate and the assumption that the population size fluctuates and that infected individuals acquire temporary immunity upon recovery. A deterministic and stochastic SIS system with continuous vaccination strategies is proposed in [20]. At the same time, it is assumed that all vaccines are effective and the disease spreads with bilinear incidence.

In models formulated through ordinary differential equations, the velocity of variation exclusively relies on the instantaneous state, implying a localized influence [21,22]. In reality, however, changes in individual behavior also depend on historical states, i.e., states prior to the current state. One method to simulate this phenomenon is through fractional-order derivatives. Fractional calculus generalizes the integer-order derivative and integral to arbitrary orders. Compared to integer-order calculus, the nonlocal characteristics of fractional calculus are more capable of accurately describing dynamic systems with features such as time dependency, path dependency, memory, and heredity [23,24]. This methodology offers a refined comprehension of the intricate interplay among diverse factors in disease transmission, proving instrumental for researchers across numerous physical contexts and facilitating successful implementations of Caputo derivatives [25,26].

Given the continuous advancements in the field of epidemiological models, this study focuses on analyzing the equilibrium point characteristics of the fractional-order SIV model after proving its non-negative boundedness and delves into its existence, uniqueness, and stability analysis. Additionally, we comprehensively consider core epidemiological factors such as fractional derivatives, neonatal immunization coverage, vaccination rates among

susceptible populations, vaccine efficacy, and public behavior effects to explore how vaccination strategies impact the dynamics of disease transmission. By meticulously examining the interactions between these parameters, we aim to uncover the actual effectiveness and potential of control strategies in containing the spread of epidemics.

Furthermore, our research involves formulating optimal control strategies specifically aimed at minimizing the number of infections while keeping costs as low as possible through control measures such as modifying the behavior of susceptible populations, optimizing vaccination rates, and enhancing treatment for infected individuals. This strategy formulation process considers the practical constraints and desired goals of disease control, striving to achieve the most optimal allocation and efficient utilization of vaccination resources under limited resources.

The organization of the rest of this paper is as follows: Section 2 introduces pertinent definitions and lemmas essential for subsequent analyses. Section 4 delves into the dynamic behaviors of model (10). Section 5 examines the stability of model (10) at its equilibrium point. Section 6 formulates the fractional-order optimal control problem and outlines the optimal control strategy's architecture. Section 7 employs numerical simulations to corroborate the theoretical findings. Lastly, Section 8 summarizes the conclusions and outlines directions for future research.

2. Mathematical Preliminaries

Definition 1 ([27]). *Given a function $f(t)$ defined on the interval (a,b), with $\mu > 0$ and n being the smallest integer greater than μ, the Caputo fractional derivative of order μ for $f(t)$ is formulated as*

$$ {}_a^C D_t^\mu f(t) = \begin{cases} \frac{1}{\Gamma(n-\mu)} \int_a^t \frac{f^{(n)}(\zeta)}{(t-\zeta)^{1+\mu-n}} d\zeta, n-1 < \mu < n \\ \frac{d^n}{dt^n} f(t), \mu = n. \end{cases} \tag{1} $$

In particular, when $0 < \mu < 1$, we can obtain

$$ {}_a^C D_t^\mu f(t) = \frac{1}{\Gamma(1-\alpha)} \int_a^t \frac{f^{'}(\zeta)}{(t-\zeta)^\mu} d\zeta. \tag{2} $$

Definition 2 ([28]). *The Mittag–Leffler function with two parameters is represented as*

$$ E_{\alpha,\theta}(u) = \sum_{i=0}^{\infty} \frac{u^i}{\Gamma(i\alpha+\theta)}, \tag{3} $$

where $\alpha > 0, \theta > 0, u \in \mathrm{C}$.

Definition 3 ([27,29]). *The Laplace transform, when applied to the Caputo fractional differentiation, can be expressed as follows:*

$$ \mathcal{L}\left\{ {}_0^C D_t^\mu f(t); s \right\} = s^\mu F(s) - \sum_{i=0}^{n-1} s^{\mu-i-1} f^{(i)}(0), \tag{4} $$

where $n-1 < \mu \leq n$. In particular, when the initial value satisfies $f^i(0) = 0, i = 0, 1, ..., n-1$, it can be obtained that

$$ \mathcal{L}\left\{ {}_0^C D_t^\mu f(t); s \right\} = s^\mu F(s). \tag{5} $$

Lemma 1 ([30]). *Let $h \in C^1(a,b]$ and $\mu \in (0,1)$:*
(i) For $\forall\, t \in [a,b]$, if $D^\mu h(t) > 0$, then $h(t)$ is monotonically increasing.
(ii) For $\forall\, t \in [a,b]$, if $D^\mu h(t) < 0$, then $h(t)$ is monotonically decreasing.

Lemma 2 ([31]). *Suppose* $\psi : [t_0, \infty) \to \mathbb{R}$ *is a continuous function, and satisfy*

$$\begin{cases} D^{\mu}\psi(t) + \lambda\psi(t) \leq \nu, \\ \psi(t_0) = \psi_0. \end{cases} \tag{6}$$

where $\mu \in (0, 1]$, $\lambda, \nu \in \mathbb{R}$, *and the initial time is* $t_0 \geq 0$. *Then there is the following inequality:*

$$\psi(t) \leq \left(\psi - \frac{\nu}{\lambda}\right) E_{\mu}(-\lambda(t - t_0)^{\mu}) + \frac{\nu}{\lambda}. \tag{7}$$

Lemma 3 ([32]). *Assuming h(t) is a continuous and differentiable function defined on the positive real numbers* $\mathbb{R}^+$, *then*

$${}_a^C D_t^{\mu}\left(h(t) - h_* - h_* ln\frac{h(t)}{h_*}\right) \leq (1 - \frac{h(t)}{h_*})\,{}_a^C D_t^{\mu} h(t), \tag{8}$$

where $h_* \in \mathbb{R}^+, \forall \mu \in (0, 1]$.

3. Model Derivation

In this section, we present a fractional-order SIV epidemic model with a non-monotonic incidence rate. This model explores the intricate interactions between susceptible, infected, and vaccinated individuals.

We initially categorize the population into three distinct compartments. The first compartment represents the susceptible individuals ($S(t)$) who are at risk of contracting the disease. The second compartment comprises the infected individuals ($I(t)$) who have already been infected and pose a risk of transmitting the disease. Lastly, the third compartment includes those who have been vaccinated and have gained immunity ($V(t)$). However, it is important to note that vaccinated individuals may experience a loss of immunity over time, which implies they may either become infected again or revert back to the susceptible compartment. In reality, vaccines rarely offer one hundred percent efficacy. As such, we incorporated the rate of immunity loss and the vaccine's effectiveness into our model to better understand their impact on the disease dynamics. The flowchart of SIV prevalence is shown in Figure 1.

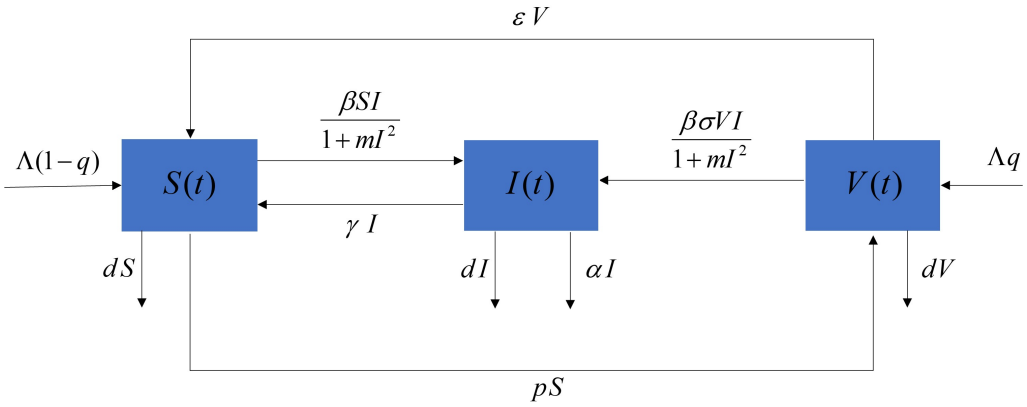

Figure 1. Disease transmission flow chart.

The SIV model incorporating vaccination strategies can be represented by the following interconnected nonlinear differential equations:

$$\begin{cases} S(t) = \Lambda(1-q) + \varepsilon V + \gamma I - (\frac{\beta I}{1+mI^2} + p + d)S \\ I(t) = \frac{\beta(S+\sigma V)}{1+mI^2} I - (\gamma + d + \alpha)I \\ V(t) = \Lambda q + pS - \frac{\beta\sigma V}{1+mI^2} I - (d+\varepsilon)V \end{cases} \tag{9}$$

The meanings of the other parameters within the model are detailed in Table 1 below.

Table 1. Model (10) parameter description.

Parameter	Description
Λ	Population supplement rate
p	Vaccination rate of susceptible populations
ε	Immune loss rate
γ	Recovery rate of infected populations
β	Contact rate
q	Vaccination rate of newborns
d	Natural mortality rate
α	Mortality rate due to disease
σ	Effectiveness of the vaccine

As we discussed earlier, compared to integer-order calculations, the nonlocal characteristics of fractional-order differential equations are more suitable for accurately describing dynamic systems with characteristics such as time dependence, path dependence, memory, and heredity. Therefore, the aforementioned ordinary differential model (9) can be further extended to the following θ-order fractional-order system. Using the definition of Caputo's fractional derivative, system (9) can be rewritten as

$$\begin{cases} {}_0^C D_t^\theta S(t) = \Lambda(1-q) + \varepsilon V + \gamma I - (\frac{\beta I}{1+mI^2} + p + d)S \\ {}_0^C D_t^\theta I(t) = \frac{\beta(S+\sigma V)}{1+mI^2} I - (\gamma + d + \alpha)I \\ {}_0^C D_t^\theta V(t) = \Lambda q + pS - \frac{\beta\sigma V}{1+mI^2} I - (d+\varepsilon)V \end{cases} \tag{10}$$

4. Model Analysis

4.1. Non-Negativity and Boundedness of Solutions

Let $\mathfrak{A}^+ = \{(S, I, V) \in \mathfrak{A} : S, I, V \in \mathcal{R}^+\}$, where $\mathcal{R}^+$ encompasses all positive real numbers.

Theorem 1. *Every vertex of system (10) lies within $\mathfrak{A}^+$, maintains non-negativity, and is uniformly bounded over $t \geq 0$.*

Proof of Theorem 1. Non-negativity: Suppose the system has an equilibrium at $X(t_i) = (S(t_i), I(t_i), V(t_i)) \in \mathfrak{A}^+$ at the initial time. From the system (10), we have

$$D_S^\theta|_{S_{t_0}=0} = \Lambda(1-q) + \varepsilon V + \gamma I \geqslant 0, \tag{11}$$

$$D_I^\theta|_{I_{t_0}=0} = 0, \tag{12}$$

$$D_V^\theta|_{V_{t_0}=0} = \Lambda q + pS \geq 0. \tag{13}$$

By Lemma 1, for $t \geq t_0$, we obtain $S(t), I(t), V(t) \geq 0$. Therefore, under the initial conditions, all the vertices of the system are finally in $\mathfrak{A}^+$.

Boundedness: View the overall population as the aggregated total of the three segments, i.e., $N(t) = S(t) + I(t) + V(t)$. Then

$$\begin{aligned} D^\theta N(t) &= D^\theta S(t) + D^\theta I(t) + D^\theta V(t) \\ &= \Lambda - dN(t) - \alpha I(t) \\ &\leqslant \Lambda - dN(t) \end{aligned} \tag{14}$$

$$\Longrightarrow D^\theta N(t) + dN(t) \leqslant \Lambda. \tag{15}$$

By Lemma 2, it follows that $N(t) \leq \left(N(t_0) - \frac{\Lambda}{d}\right) E_\theta\left(-d(t-t_0)^\theta\right) + \frac{\Lambda}{d}$, when $t \longrightarrow \infty$, $N(t) \geq \frac{\Lambda}{d}$ holds true. Thus, the proof of boundedness is complete. In conclusion, the proof of non-negative boundedness is complete. □

4.2. Existence and Uniqueness of Solutions

The subsequent lemma serves as the foundation for verifying the existence and uniqueness of the solution.

Lemma 4 ([32]). *Consider the fractional-order system presented below:*

$$D^\mu h(t) = g(t, y), \quad y(t_0) = y_0, \text{ and } t_0 > 0.$$

where $\mu \in (0, 1]$, $g : [t_0, +\infty) \times \mathfrak{A} \to \mathbb{R}^n$. If $g(t, x)$ satisfies the Lipschitz condition with respect to y, that is, there exists a constant $L \geqslant 0$ such that $|g(t, y_1) - g(t, y_2)| \leqslant L|y_1 - y_2|$ for all $(t, y_1), (t, y_2) \in \mathcal{N}$, then for the system there exists a unique solution in $[t_0, \infty) \times \mathfrak{A}$.

Theorem 2. *Given any initial condition $\mathfrak{X}_{t_0} = (S_{t_0}, I_{t_0}, V_{t_0})$ within the positive space $\mathfrak{A}^+$, the system (10) possesses a unique solution $\mathfrak{X}(t) = (\bar{S}(t), \bar{I}(t), \bar{V}(t))$ that persists within $\mathfrak{A}^+$ for all later times $t > t_0$.*

Proof of Theorem 2. Consider the region $\mathfrak{A}^+ \times [t_0, t_1]$, where $\mathfrak{A}^+ = \{(S, I, V) \in \mathbb{R}^3 : \max\{|S|, |I|, |V|\} \leq k\}$. Let t_1 be a finite number. Denote $\mathfrak{X}(t) = (S(t), I(t), V(t))$ and $\bar{\mathfrak{X}}(t) = (\bar{S}(t), \bar{I}(t), \bar{V}(t))$, abbreviated as $\mathfrak{X}(t) = \mathfrak{X}$ and $\bar{\mathfrak{X}}(t) = \bar{\mathfrak{X}}$.

Suppose $P(\mathfrak{X}) = (P_1(\mathfrak{X}), P_2(\mathfrak{X}), P_3(\mathfrak{X}))$, where

$$P_1(\mathfrak{X}) = \Lambda(1-q) + \varepsilon V + \gamma I - \left(\frac{\beta I}{1+mI^2} + p + d\right)S, \tag{16}$$

$$P_2(\mathfrak{X}) = \frac{\beta(S+\sigma V)}{1+mI^2} I - (\gamma + d + \alpha)I, \tag{17}$$

$$P_3(\mathfrak{X}) = \Lambda q + pS - \frac{\beta\sigma I}{1+mI^2} V - (d+\varepsilon)V. \tag{18}$$

For $\forall \mathfrak{X}, \bar{\mathfrak{X}} \in \mathfrak{A}^+$,

$$\begin{aligned}
&\|P(\mathfrak{X}) - P(\bar{\mathfrak{X}})\| \\
&= |P_1(\mathfrak{X}) - P_1(\bar{\mathfrak{X}})| + |P_2(\mathfrak{X}) - P_2(\bar{\mathfrak{X}})| + |P_3(\mathfrak{X}) - P_3(\bar{\mathfrak{X}})| \\
&= \left|\Lambda(1-q) + \varepsilon V + \gamma I - \left(\frac{\beta I}{1+mI^2} + p + d\right)S\right. \\
&\left. - \left(\Lambda(1-q) + \varepsilon\bar{V} + \gamma\bar{I} - \left(\frac{\beta\bar{I}}{1+m\bar{I}^2} + p + d\right)\right)\bar{S}\right| \\
&+ \left|\frac{\beta(S+\sigma V)}{1+mI^2} I - (\gamma+d+\alpha)I - \left(\frac{\beta(\bar{S}+\sigma\bar{V})}{1+m\bar{I}^2}\bar{I} - (\gamma+d+\alpha)\bar{I}\right)\right| \\
&+ \left|\Lambda q + pS - \frac{\beta\sigma I}{1+mI^2} V - (d+\varepsilon)V - \left(\Lambda q + p\bar{S} - \frac{\beta\sigma\bar{I}}{1+m\bar{I}^2}\bar{V} - (d+\varepsilon)\bar{V}\right)\right| \\
&\leq |V - \bar{V}| + \gamma|I - \bar{I}| + (\gamma + d + \alpha)|I - \bar{I}| + p\left|S - \bar{S}\right| + (d+\varepsilon)|V - \bar{V}| \\
&+ 2\beta\left|\frac{SI}{1+mI^2} - \frac{\bar{S}\bar{I}}{1+m\bar{I}^2}\right| + (p+d)\left|S - \bar{S}\right| + 2\beta\left|\frac{\sigma IV}{1+mI^2} - \frac{\sigma\bar{I}\bar{V}}{1+m\bar{I}^2}\right| \\
&\leq (2p + d + 2\beta k)\left|S - \bar{S}\right| + (2\gamma + d + \alpha + 2\beta\sigma k)|I - \bar{I}| + (2\varepsilon + d)|V - \bar{V}| \\
&\leq M_1\left|S - \bar{S}\right| + M_2|I - \bar{I}| + M_3|V - \bar{V}| \\
&\leq M|\mathfrak{X} - \bar{\mathfrak{X}}|
\end{aligned} \tag{19}$$

where

$$\begin{aligned} M &= \max\{M_1, M_2, M_3\}, \\ M_1 &= 2p + d + 2\beta k, \\ M_2 &= 2\gamma + d + \alpha + 2\beta\sigma k, \\ M_3 &= 2\varepsilon + d. \end{aligned}$$

Hence, based on Lemma 4, the uniqueness of the system's solution is made more unique by the fact that $P(\mathfrak{X})$ satisfies Lipschitz's condition. □

4.3. Existence of Equilibria

To ascertain the equilibrium state of system (10), we set the expressions on the right side of the equations to null, effectively converting the system (10) into a form:

$$\begin{cases} \Lambda(1-q) + \varepsilon V + \gamma I - (\frac{\beta_I}{1+mI^2} + p + d)S = 0 \\ \frac{\beta(S+\sigma V)}{1+mI^2} I - (\gamma + d + \alpha)I = 0 \\ \Lambda q + pS - \frac{\beta\sigma I}{1+mI^2} V - (d+\varepsilon)V = 0 \end{cases} \tag{20}$$

After simplification and calculation, two equilibrium points are obtained: the disease-free equilibrium point $E_0 = (\frac{\Lambda(\varepsilon+d(1-q))}{d(d+p+\varepsilon)}, 0, \frac{\Lambda(dq+p)}{d(d+p+\varepsilon)})$ and the endemic equilibrium point $E_e = (S_e, I_e, V_e)$, where

$$S_e = \frac{d(1+mI_e^2)(\gamma+d+\alpha) - \beta\sigma(\Lambda - I_e(d+\alpha))}{\beta d(1-\sigma)},$$

$$V_e = \frac{\beta(\Lambda - I_e(d+\alpha)) - d(\gamma 1 + d + \alpha)(1+mI_e^2)}{\beta d(1-\sigma)},$$

and I_e can represent it with the equation

$$AI_e{}^4 + BI_e{}^3 + CI_e{}^2 + DI_e + E = 0, \tag{21}$$

where

$$\begin{aligned} A =& dm^2(\gamma+d+\alpha)(p+d+\varepsilon), \\ B =& \beta m((d+\alpha)(d+(p+d)\sigma+\varepsilon) + d\gamma\sigma), \\ C =& (d+\alpha)\Big(\beta^2\sigma + 2dm(p+d+\varepsilon)\Big) + 2d\gamma m(p+d+\varepsilon) \\ & - \beta\Lambda m((p+d)\sigma + d(1-q)(1-\sigma) + \varepsilon), \\ D =& \beta((d+\alpha)(d+(p+d)\sigma+\varepsilon) - \beta\sigma\Lambda + d\gamma\sigma), \\ E =& d(\gamma+d+\alpha)(p+d+\varepsilon) - \beta\Lambda((p+d)\sigma + d(1-q)(1-\sigma) + \varepsilon). \end{aligned}$$

4.4. Basic Reproduction Number

The basic reproduction number is a parameter that describes the transmission capacity of a certain infectious disease within a susceptible population [33]. It signifies the anticipated quantity of additional infections that can arise from a single infected person throughout their contagious duration at the very beginning of a disease outbreak when all members of the population are susceptible. This paper calculates the basic reproduction number through the next-generation matrix method, drawing on the pioneering approach established by Driessche and Watmough [34,35].

In this system, $\mathcal{F}$ signifies the growth rate of secondary infections within the infected compartment, and $\mathcal{V}$ represents the reduction rate due to disease progression, death, and recovery within the infected compartment.

$$\mathcal{F} = \frac{\beta(S+\sigma V)}{1+mI^2} I, \mathcal{V} = (\gamma + d + \alpha)I.$$

Hence, the Jacobian matrices of $\mathcal{F}$ and $\mathcal{V}$ evaluated at the disease-free equilibrium point E_0 are presented as follows:

$$F = \beta\left(\frac{\Lambda\varepsilon + d(1-q)}{d(d+\varepsilon+p)} + \frac{\sigma\Lambda(dq+p)}{d(d+\varepsilon+p)}\right), V = \gamma + d + \alpha.$$

Therefore,

$$\begin{aligned} R_0 &= \rho_0(FV^{-1}) \\ &= \frac{\beta\Lambda(\varepsilon + d - (1-\sigma)dq + \sigma p)}{d(d+\varepsilon+p)(\gamma+d+\alpha)}. \end{aligned} \tag{22}$$

5. Stability Analysis of the Equilibria

This section delves into the stability analysis of both the disease-free equilibrium and the endemic equilibrium, examining them from two distinct perspectives: locally asymptotically stable and globally asymptotically stable. First, the Jacobian matrix of the system (10) at an arbitrary point $X = (S, I, V)$ is constructed as follows:

$$J(S,I,V) = \begin{bmatrix} -(\frac{\beta I}{1+mI^2} + p + d) & \gamma & \varepsilon \\ \frac{\beta I}{1+mI^2} & \frac{\beta(S+\sigma V)(1-mI^2)}{(1+mI^2)^2} - (\gamma+d+\alpha) & \frac{\beta\sigma I}{1+mI^2} \\ p & -\frac{\beta\sigma V(1-mI^2)}{(1+mI^2)^2} & -\frac{\beta\sigma I}{1+mI^2} - d - \varepsilon \end{bmatrix}$$

Theorem 3. *If $R_0 < 1$, then the disease-free equilibrium point E_0 of the system (10) is locally asymptotically stable.*

Proof of Theorem 3. At the disease-free equilibrium E_0 of the system (10), the Jacobian matrix is

$$\begin{aligned} J(S_0, I_0, V_0) &= \begin{bmatrix} -(p+d) & \gamma & \varepsilon \\ 0 & \beta(S_0+\sigma V_0)(-(\gamma+d+\alpha) & 0 \\ p & -\beta\sigma V_0 & -d-\varepsilon \end{bmatrix} \\ &= \begin{bmatrix} -(p+d) & \gamma & \varepsilon \\ 0 & \frac{\beta\Lambda[\varepsilon+d+\sigma p-(1-\sigma)dq]}{d(p+d+\varepsilon)}(-(\gamma+d+\alpha) & 0 \\ p & -\frac{\beta\sigma\Lambda(dq+p)}{d(p+d+\varepsilon)} & -d-\varepsilon \end{bmatrix} \end{aligned}$$

The corresponding characteristic equation at E_0 is

$$\begin{aligned} |\lambda E - J(E_0)| = &\left(\lambda - \frac{\beta\Lambda(\varepsilon+d+\sigma p-(1-\sigma)dq)}{d(p+d+\varepsilon)} + \gamma + d + \alpha\right) \\ &((\lambda+p+d)(\lambda+d+\varepsilon) - \varepsilon p) = 0. \end{aligned} \tag{23}$$

Through observation of the characteristic equation, one can find that at $E0$, one of the eigenvalues is

$$\begin{aligned}\lambda_1 &= \frac{\beta\Lambda(\varepsilon + d + \sigma p - (1-\sigma)dq)}{d(p+d+\varepsilon)} - (\gamma + d + \alpha) \\ &= (\gamma + d + \alpha)(R_0 - 1).\end{aligned} \tag{24}$$

When $R_0 < 1$, it is evident that $\lambda_1 < 0$. It can be found that λ_2 and λ_3 satisfy the equation:

$$(\lambda + p + d)(\lambda + d + \varepsilon) - \varepsilon p = 0. \tag{25}$$

After simplification, it becomes

$$\lambda^2 + (p + 2d + \varepsilon)\lambda + pd + d^2 + d\varepsilon = 0. \tag{26}$$

It is easy to know $p + 2d + \varepsilon > 0$ and $pd + d^2 + d\varepsilon > 0$; then the Routh–Hurwitz conditions are satisfied, confirming that under the condition $R_0 < 1$, the point E_0 is locally asymptotically stable. □

Theorem 4. *If $R_0 > 1$, then the endemic equilibrium point E_e of the system (10) is locally asymptotically stable if $a_2 > 0, a_1 > 0, a_0 > 0$ and $a_2 a_1 - a_0 > 0$, where*

$$\begin{aligned}
a_2 =& \gamma + 3d + \varepsilon + p + \alpha - \frac{(1 - mI_e^2)(\gamma + d + \alpha) - \beta I_e(\sigma - 1)}{1 + mI_e^2}, \\
a_1 =& (d + p + \frac{\beta I_e}{1 + mI_e^2})(d + \varepsilon + \frac{\beta I_e}{1 + mI_e^2}) - \varepsilon p + \left(d + \alpha - \frac{\beta S_e(1 - mI_e^2)}{(1 + mI_e^2)^2}\right) \\
& \left(2d + \varepsilon + p + \frac{\beta I_e(\sigma + 1)}{1 + mI_e^2}\right) - \left(\frac{\beta\sigma V_e(1 - mI_e^2)}{(1 + mI_e^2)^2} - \gamma\right)(p + d + \varepsilon) \\
& + \frac{\beta\sigma I_e}{1 + mI_e^2}\left(\frac{\beta V_e(1 - mI_e^2)}{(1 + mI_e^2)^2} - \gamma\right) + \frac{\beta\sigma V_e(1 - mI_e^2)}{(1 + mI_e^2)^2} - \gamma, \\
a_0 =& d + \alpha - \frac{\beta S_e(1 - mI_e^2)}{(1 - mI_e^2)^2}\left((d + p + \frac{\beta I_e}{1 + mI_e^2})(d + \varepsilon + \frac{\beta\sigma I_e}{1 + mI_e^2}) - \varepsilon p\right) \\
& - \left(\frac{\beta\sigma V_e(1 - mI_e^2)}{(1 + mI_e^2)^2} - \gamma\right)(p + d + \varepsilon)d - \frac{\beta\sigma I_e}{1 + mI_e^2}\left(\frac{\beta V_e(1 - mI_e^2)}{(1 + mI_e^2)^2} - \gamma\right)d.
\end{aligned}$$

Proof of Theorem 4. At the endemic equilibrium point E_e of the system (10), the Jacobian matrix is

$$J(S_e, I_e, V_e) = \begin{bmatrix} -(\frac{\beta I_e}{1+mI_e^2} + p + d) & \gamma & \varepsilon \\ \frac{\beta I_e}{1+mI_e^2} & \frac{\beta(S_e + \sigma V_e)(1-mI_e^2)}{(1+mI_e^2)^2} - (\gamma + d + \alpha) & \frac{\beta\sigma I_e}{1+mI_e^2} \\ p & -\frac{\beta\sigma V_e(1-mI_e^2)}{(1+mI_e^2)^2} & -\frac{\beta\sigma I}{1+mI_e^2} - d - \varepsilon \end{bmatrix}.$$

Subsequently, the characteristic equation of the aforementioned matrix is expressed as

$$\lambda^3 + a_2\lambda^2 + a_1\lambda + a_0 = 0, \tag{27}$$

where

$$\begin{aligned}
a_2 =&\gamma + 3d + \varepsilon + p + \alpha - \frac{(1 - mI_e^2)(\gamma + d + \alpha) - \beta I_e(\sigma - 1)}{1 + mI_e^2};\\
a_1 =&(d + p + \frac{\beta I_e}{1 + mI_e^2})(d + \varepsilon + \frac{\beta I_e}{1 + mI_e^2}) - \varepsilon p + \left(d + \alpha - \frac{\beta S_e(1 - mI_e^2)}{(1 + mI_e^2)^2}\right)\\
&\left(2d + \varepsilon + p + \frac{\beta I_e(\sigma + 1)}{1 + mI_e^2}\right) - \left(\frac{\beta\sigma V_e(1 - mI_e^2)}{(1 + mI_e^2)^2} - \gamma\right)(p + d + \varepsilon)\\
&+ \frac{\beta\sigma I_e}{1 + mI_e^2}\left(\frac{\beta V_e(1 - mI_e^2)}{(1 + mI_e^2)^2} - \gamma\right) + \frac{\beta\sigma V_e(1 - mI_e^2)}{(1 + mI_e^2)^2} - \gamma;\\
a_0 =&d + \alpha - \frac{\beta S_e(1 - mI_e^2)}{(1 - mI_e^2)^2}\left((d + p + \frac{\beta I_e}{1 + mI_e^2})(d + \varepsilon + \frac{\beta\sigma I_e}{1 + mI_e^2}) - \varepsilon p\right)\\
&- \left(\frac{\beta\sigma V_e(1 - mI_e^2)}{(1 + mI_e^2)^2} - \gamma\right)(p + d + \varepsilon)d - \frac{\beta\sigma I_e}{1 + mI_e^2}\left(\frac{\beta V_e(1 - mI_e^2)}{(1 + mI_e^2)^2} - \gamma\right)d.
\end{aligned}$$

According to the Routh–Hurwitz stability criteria, if $a_2 > 0, a_1 > 0, a_0 > 0$ and $a_2a_1 - a_0 > 0$, the endemic equilibrium point E_e is locally asymptotically stable. □

Theorem 5. *If* $R_0 < 1$, $\frac{d}{\varepsilon} > \frac{dq+p}{\varepsilon d(1-q)}$, *and* $\frac{d}{p} > \frac{\varepsilon d(1-q)}{dq+p}$, *then the disease-free equilibrium point* E_0 *of the system (10) is globally asymptotically stable.*

Proof of Theorem 5. Let us consider the Lyapunov function as

$$L_1(S, I, V) = S - S_0 - S_0 ln\frac{S}{S_0} + I + V - V_0 - V_0 ln\frac{V}{V_0}.$$

Then, by Lemma 3, we have

$$\begin{aligned}
D^\theta L_1 \leq&(1 - \frac{S_0}{S})D^\theta S + D^\theta I + (1 - \frac{V_0}{V})D^\theta V\\
=&(1 - \frac{S}{S_0})\left(\Lambda(1 - q) + \varepsilon V + \gamma I - (\frac{\beta I}{1 + mI^2} + p + d)S\right)\\
&+ \frac{\beta(S + \sigma V)}{1 + mI^2}I - (\gamma + d + \alpha)I\\
&+ (1 - \frac{V}{V_0})\left(\Lambda q + pS - \frac{\beta\sigma I}{1 + mI^2}V - (d + \varepsilon)V\right)\\
=&\Lambda - d(S + I + V) - \alpha I - \frac{S_0}{S}\left(\Lambda(1 - q) + \varepsilon V + \gamma I - (\frac{\beta I}{1 + mI^2} + p + d)S\right)\\
&- \frac{V_0}{V}\left(\Lambda q + pS - \frac{\beta\sigma I}{1 + mI^2}V - (d + \varepsilon)V\right)
\end{aligned} \tag{28}$$

For $R_0 < 1$, the steady-state equation at the equilibrium point is

$$\Lambda(1 - q) = (p + d)S_0 - \varepsilon V_0, \tag{29}$$

$$\Lambda q = (d + \varepsilon)V_0 - pS_0, \tag{30}$$

Then

$$\begin{aligned} D^\theta L_1 \leq & dS_0 + dV_0 - d(S+I+V) - \alpha I - \frac{S_0}{S}\gamma I \\ & + \frac{\beta I}{1+mI^2}S_0 + \frac{\beta\sigma I}{1+mI^2}V_0 - \frac{S_0}{S}\varepsilon V + (p+d)S_0 - \frac{V_0}{V}pS \\ & + (d+\varepsilon)V_0 - (p+d)\frac{S_0^2}{S} + \varepsilon\frac{S_0V_0}{S}(d+\varepsilon)\frac{V_0^2}{V} + p\frac{S_0V_0}{V} \\ \leq & (dS_0 - \varepsilon V_0)(2 - \frac{S}{S_0} - \frac{S_0}{S}) + (dV_0 - pS_0)(2 - \frac{V}{V_0} - \frac{V_0}{V}) \\ & + pS_0(3 - \frac{S_0}{S} - \frac{V}{V_0} - \frac{V_0S}{VS_0}) + \varepsilon V_0(3 - \frac{S}{S_0} - \frac{V_0}{V} - \frac{VS_0}{V_0S}) \end{aligned} \tag{31}$$

Since the arithmetic mean consistently exceeds the geometric mean, then $D^\theta L_1 \leq 0$ holds if and only if $dS_0 - \varepsilon V_0 > 0$ and $dV_0 - pS_0 > 0$, i.e., $\frac{d}{\varepsilon} > \frac{dq+p}{\varepsilon d(1-q)}$and $\frac{d}{p} > \frac{\varepsilon d(1-q)}{dq+p}$, where $D^\theta L_1 = 0$ if and only if $S = S_0, I = I_0, V = V_0$. In line with the Lyapunov–LaSalle asymptotic stability theorem [36,37], E_0 is globally asymptotically stable. □

Theorem 6. *If $R_0 > 1$, $dS_e - \varepsilon V_e > 0$ and $dV_e - pS_e > 0$, then the endemic equilibrium point E_e of the system (10) is globally asymptotically stable.*

Proof of Theorem 6. Let us consider the Lyapunov function as

$$L_2(S,I,V) = S - S_e - S_e ln\frac{S}{S_e} + I - I_e - I_e ln\frac{I}{I_e} + V - V_e - V_e ln\frac{V}{V_e}.$$

Then, by Lemma 3, we have

$$\begin{aligned} D^\theta L_2 \leq & (1 - \frac{S_e}{S})D^\theta S + (1 - \frac{I_e}{I})D^\theta I + (1 - \frac{V_e}{V})D^\theta V \\ = & \Lambda - d(S+I+V) - \alpha I - \frac{S_e}{S}\left(\Lambda(1-q) + \varepsilon V + \gamma I - (\frac{\beta I}{1+mI^2} + p + d)S\right) \\ & - \frac{I_e}{I}\left(\frac{\beta(S+\sigma V)}{1+mI^2}I - (\gamma + d + \alpha)I\right) - \frac{V_e}{V}\left(\Lambda q + pS - \frac{\beta\sigma I}{1+mI^2}V - (d+\varepsilon)V\right) \end{aligned} \tag{32}$$

For $R_0 > 1$, the steady-state equation at the equilibrium point is

$$\Lambda(1-q) = (\frac{\beta I_e}{1+mI_e^2} + p + d)S_e - \varepsilon V_e - \gamma I_e, \tag{33}$$

$$\gamma = \frac{\beta(S_e + \sigma V_e)}{1+mI_e^2} - (d+\alpha), \tag{34}$$

$$\Lambda q = \frac{\beta\sigma I_e}{1+mI_e^2}V_e + (d+\varepsilon)V_e - pS_e. \tag{35}$$

Then

$$\begin{aligned}
D^{\theta}L_2 \leq & d(S_e+I_e+V_e)+\alpha I_e-d(S+I+V)-\alpha I \\
& -(p+d)\frac{S_e^2}{S}+\varepsilon\frac{S_eV_e}{S}+\frac{\beta\sigma V_eI_e}{1_mI_e^2}\frac{S_e}{S}-(d+\alpha)\frac{S_eI_e}{S}-\varepsilon V\frac{S_e}{S} \\
& -\left(\frac{\beta(S_e+\sigma V_e)}{1+mI_e^2-(d+\alpha)}\right)\frac{S_eI}{S}+(\frac{\beta I}{1+mI^2})S_e \\
& -\frac{\beta(S+\sigma V)}{1+mI^2}I_e+\frac{\beta(S_e+\sigma V_e)}{1+mI_e^2}I_e \\
& -(\frac{\beta\sigma I_e}{1+mI^2}+d+\varepsilon)\frac{V_e^2}{V}+p\frac{V_eS_e}{V}-p\frac{V_eS}{V}+(\frac{\beta\sigma I}{1+mI^2}+p+d)V_e \\
\leq & (dS_e-\varepsilon V_e)(2-\frac{S}{S_e}-\frac{S_e}{S})+(dV_e-pS_e)(2-\frac{V}{V_e}-\frac{V_e}{V}) \\
& +pS_e(3-\frac{S_e}{S}-\frac{V}{V_e}-\frac{V_eS}{VS_e})+\varepsilon V_e(3-\frac{S}{S_e}-\frac{V_e}{V}-\frac{VS_e}{V_eS})
\end{aligned} \tag{36}$$

Since the arithmetic mean consistently exceeds the geometric mean, then $D^{\theta}L_2 \leq 0$ holds if and only if $dS_e - \varepsilon V_e > 0$ and $dV_e - pS_e > 0$, where $D^{\theta}L_2 = 0$ if and only if $S = S_e, I = I_e, V = V_e$. In line with the Lyapunov–LaSalle asymptotic stability theorem [36,37], E_e is globally asymptotically stable. □

6. Fractional Optimal Control

In this section, a comprehensive control strategy is proposed for the aforementioned infectious disease model, striving to reduce the disease's effects while also maintaining control expenditures at a minimum. The goal of these control measures is to lower the incidence of infections within the population, which necessitates the creation of an optimal control problem to realize the desired outcome. During the epidemic transmission process, by changing the behaviors of susceptible individuals, such as maintaining social distance, improving awareness, and prevention of the disease, the rate at which susceptible individuals become infected can be decreased, which is represented by the control variable $u_1(t)$. By increasing the vaccination rate among susceptible individuals, for instance, through promoting vaccination campaigns, offering vaccine subsidies, or expanding vaccine supply, we can significantly reduce their risk of contracting the disease. This is represented by the control variable $u_2(t)$. $u_3(t)$, on the other hand, signifies the extent of therapeutic measures undertaken for infected individuals (those who have already contracted the disease) at time t. These measures may encompass pharmacological interventions (such as medication and vaccine therapy) and physical segregation practices (like isolation wards and home quarantine). Upon enhancing the aforementioned three control strategies, System (10) undergoes the following modification:

$$\begin{cases}
{}_0^C D_t^{\theta}S(t) = \Lambda(1-q)+\varepsilon V+(\gamma+u_3(t))I-(1-u_1(t))\dfrac{\beta SI}{1+mI^2}-(p+u_2(t)+d)S \\
{}_0^C D_t^{\theta}I(t) = (1-u_1(t))\dfrac{\beta SI}{1+mI^2}+\dfrac{\beta\sigma VI}{1+mI^2}-(\gamma+u_3(t)+d+\alpha)I \\
{}_0^C D_t^{\theta}V(t) = \Lambda q+(p+u_2(t))S-\dfrac{\beta\sigma V}{1+mI^2}I-(d+\varepsilon)V
\end{cases} \tag{37}$$

In this scenario, the initial conditions, which are non-negative, are provided as

$$S(0) = S_0, I(0) = I_0, V(0) = V_0.$$

The designated control set is clearly outlined as

$$U = \{(u_1,u_2,u_3) | u_i \text{ is Lebesgue measurable on } [0,1], i = 1,2,3\}.$$

Our overarching control objective involves minimizing both the proportion of infected individuals within the population and the associated expenses incurred through the utilization of control variables $u_i(t)$ (where $i = 1, 2, 3$). Therefore, we define the objective function

$$J(u_1, u_2, u_3) = \int_0^T (B_1 I + \frac{1}{2} C_1 u_1^2 + \frac{1}{2} C_2 u_2^2 + \frac{1}{2} C_3 u_3^2) dt \tag{38}$$

subject to the model (37) with initial conditions, where T represents the control period, B_1 denotes the weight for infected individuals, and C_1, C_2, and C_3 serve as the weighting constants, each corresponding to the financial burden associated with implementing the respective control measures. $\frac{1}{2} C_1 u_1^2$, $\frac{1}{2} C_2 u_2^2$, and $\frac{1}{2} C_3 u_3^2$ are the implementation costs for these three measures, respectively. Our main objective is to determine the optimal control $U^* = (u_1^*, u_2^*, u_3^*) \in U$ for the system, guaranteeing that the objective function reaches its minimal value, that is,

$$J(u_1^*, u_2^*, u_3^*) = \min_{u \in U} J(u_1, u_2, u_3)$$

Next, we apply Pontryagin's maximum principle [38] to solve the optimal control problem. First of all, we need to prove that the optimal solution exists for the system (37).

Theorem 7. *There exists an optimal control solution* (u_1^*, u_2^*, u_3^*) *such that*

$$J(u_1^*, u_2^*, u_3^*) = \min_{u \in U} J(u_1, u_2, u_3),$$

subject to the fractional system (37).

Proof of Theorem 7. From the aforementioned analysis of the model (10) and the results in [39], the existence of the optimal control U^* is contingent upon the fulfillment of the following conditions:

(i) The set of control U and the corresponding set of state variables are non-empty;

(ii) U is closed and convex;

(iii) The right side of the system (37) is bounded by a linear function with the control and state variables;

(iv) The integrand of the objective function

$$L(I, u_1, u_2, u_3) = B_1 I + \frac{1}{2} C_1 u_1^2 + \frac{1}{2} C_2 u_2^2 + \frac{1}{2} C_3 u_3^2$$

exhibits convexity within the set U;

(v) There exist constants $K_1, K_2 > 0$ and $Q > 1$ such that the integrand $L(I, u_1, u_2, u_3)$ satisfies

$$L(I, u_1, u_2, u_3) \geq K_1 (|u_1|^2 + |u_2|^2 + |u_3|^2)^{\frac{Q}{2}} - K_2.$$

□

To derive the optimal control solution, we introduce Lagrangian function

$$L(I, u_1, u_2, u_3) = B_1 I + \frac{1}{2} C_1 u_1^2 + \frac{1}{2} C_2 u_2^2 + \frac{1}{2} C_3 u_3^2 \tag{39}$$

and Hamiltonian function

$$H(S, I, V, u, \lambda) = L(I, u_1, u_2, u_3) + \lambda_1 {}_0^C D_t^\theta S(t) + \lambda_2 {}_0^C D_t^\theta I(t) + \lambda_3 {}_0^C D_t^\theta V(t), \tag{40}$$

where $\lambda_i(t)$ for $i = 1,2,3$ are the adjoint variables. By applying Pontryagin's maximum principle, we derive the adjoint variable equation and the transversal condition as indicated below:

$$\begin{aligned}
D^\theta\lambda_1(t) &= -\frac{\partial H}{\partial S} = -\left(\frac{(1-u_1(t))\beta I}{1+mI^2} + (p+u_2(t)+d)\right)\lambda_2 \\
&\quad - \frac{(1-u_1(t))\beta I}{1+mI^2}\lambda_2 - (p+u_2(t))\lambda_3 \\
D^\theta\lambda_2(t) &= -\frac{\partial H}{\partial I} = -B_1 - \left(\gamma + u_3(t) - \frac{(1-u_1(t))\beta S(1-mI^2)}{(1+mI^2)^2}\right)\lambda_1 \\
&\quad - \left(\frac{(1-u_1(t))\beta S + \beta\sigma V(1-mI^2)}{(1+mI^2)^2} - (\gamma + u_3(t) + d + \alpha)\right)\lambda_2 \\
&\quad + \frac{\beta\sigma V(1-mI^2)}{(1+mI^2)^2}\lambda_3 \\
D^\theta\lambda_3(t) &= -\frac{\partial H}{\partial V} = -\varepsilon\lambda_1 - \frac{\beta\sigma I}{1+mI^2}\lambda_2 + (\frac{\beta\sigma I}{1+mI^2} - d - \varepsilon)\lambda_3
\end{aligned} \tag{41}$$

satisfying transversality conditions

$$\lambda_i(T) = 0, i = 1,2,3.$$

To proceed, let us designate $\bar{S},\bar{I},\bar{V}$ as the optimal values corresponding to the variables S, I, V. Additionally, let us acknowledge $\bar{\lambda}_1, \bar{\lambda}_2, \bar{\lambda}_3$ as the solutions to Equation (41). With these clarifications in mind, we are now poised to present the subsequent theorem.

Theorem 8. *Consider U^* as the optimal value for the control parameter U; hence, U^* can be expressed as the equations:*

$$\begin{cases} u_1^* = \max\{0, \min\{\frac{\beta\bar{S}\bar{I}(\bar{\lambda}_2-\bar{\lambda}_1)}{c_1(1+m\bar{I}^2)}, 1\}\} \\ u_2^* = \max\{0, \min\{\frac{\bar{S}(\bar{\lambda}_1-\bar{\lambda}_3)}{c_2}, 1\}\} \\ u_3^* = \max\{0, \min\{\frac{\bar{I}(\bar{\lambda}_2-\bar{\lambda}_1)}{c_3}, 1\}\} \end{cases} \tag{42}$$

Proof of Theorem 8. To derive the characteristic equation of optimal control U^*, proceed by solving the equations:

$$\begin{cases} \frac{\partial H}{\partial u_1} = c_1u_1^* + \frac{\beta\bar{S}\bar{I}}{1+m\bar{I}^2}\bar{\lambda}_1 - \frac{\beta\bar{S}\bar{I}}{1+m\bar{I}^2}\bar{\lambda}_2 = 0 \\ \frac{\partial H}{\partial u_2} = c_2u_2^* - \bar{S}\bar{\lambda}_1 + \bar{S}\bar{\lambda}_3 = 0 \\ \frac{\partial H}{\partial u_3} = c_3u_3^* + \bar{I}\bar{\lambda}_1 - \bar{I}\bar{\lambda}_2 = 0 \end{cases}$$

Therefore,

$$u_1^* = \frac{\beta\bar{S}\bar{I}(\bar{\lambda}_2-\bar{\lambda}_1)}{c_1(1+m\bar{I}^2)}; u_2^* = \frac{\bar{S}(\bar{\lambda}_1-\bar{\lambda}_3)}{c_2}; u_3^* = \frac{\bar{I}(\bar{\lambda}_2-\bar{\lambda}_1)}{c_3}.$$

The optimal control solution U^* can be expressed as

$$u_1^* = \begin{cases} 0, & \frac{\beta \bar{S}\bar{I}(\bar{\lambda}_2 - \bar{\lambda}_1)}{c_1(1+m\bar{I}^2)} \leq 0, \\ \frac{\beta \bar{S}\bar{I}(\bar{\lambda}_2 - \bar{\lambda}_1)}{c_1(1+m\bar{I}^2)}, & 0 < \frac{\beta \bar{S}\bar{I}(\bar{\lambda}_2 - \bar{\lambda}_1)}{c_1(1+m\bar{I}^2)} < 1, \\ 1, & \frac{\beta \bar{S}\bar{I}(\bar{\lambda}_2 - \bar{\lambda}_1)}{c_1(1+m\bar{I}^2)} \geq 1. \end{cases}$$

$$u_2^* = \begin{cases} 0, & \frac{\bar{S}(\bar{\lambda}_1 - \bar{\lambda}_3)}{c_2} \leq 0, \\ \frac{\bar{S}(\bar{\lambda}_1 - \bar{\lambda}_3)}{c_2}, & 0 < \frac{\bar{S}(\bar{\lambda}_1 - \bar{\lambda}_3)}{c_2} < 1, \\ 1, & \frac{\bar{S}(\bar{\lambda}_1 - \bar{\lambda}_3)}{c_2} \geq 1. \end{cases}$$

$$u_3^* = \begin{cases} 0, & \frac{\bar{I}(\bar{\lambda}_2 - \bar{\lambda}_1)}{c_3} \leq 0, \\ \frac{\bar{I}(\bar{\lambda}_2 - \bar{\lambda}_1)}{c_3}, & 0 < \frac{\bar{I}(\bar{\lambda}_2 - \bar{\lambda}_1)}{c_3} < 1, \\ 1, & \frac{\bar{I}(\bar{\lambda}_2 - \bar{\lambda}_1)}{c_3} \geq 1. \end{cases}$$

given that the control variable (U) is bounded. This concludes the demonstration of Theorem 8. □

7. Numerical Simulation

Given the intricacy of obtaining analytical solutions, the use of numerical methods becomes essential. This section utilizes the fractional Adams–Bashforth–Moulton method [40] and particle swarm optimization [41] for numerical experimentation via MATLAB R2023(b), aiming to validate some of the theoretical findings discussed earlier in the paper. Additionally, numerous numerical simulations have been carried out, encompassing a wide range of biologically feasible parameter spaces, yielding a comprehensive array of dynamic outcomes across various scenarios. With the scale for population set at 1 million individuals and the time scale at one day, the model's parameters are defined as follows: $\alpha = 0.15, \beta = 0.45, d = 0.15, \gamma = 0.25, p = 0.2, q = 0.4, \sigma = 0.06, \Lambda = 0.35, \varepsilon = 0.05$, $m = 0.3$, and the initial populations in each compartment are set as $S(0) = 4.5, I(0) = 0.2$, $V(0) = 0.3$.

7.1. Numerical Simulation without Control Measures

In this subsection, we present numerical results for a fractional system. Figures 2 and 3 showcase the dynamic behavior of the susceptible, infected, and vaccinated classes across various fractional orders θ. Figure 2 demonstrates that when the parameter takes the aforementioned value, which corresponds to $R_0 = 0.7426$, the disease-free equilibrium point E_0 is locally asymptotically stable, validating Theorem 3. Additionally, it is evident that the fractional order θ holds a pivotal position in governing the dynamics of these three distinct compartments and influences the duration required for each to attain stability. Within the community, an augmentation in the value of θ is observed to be directly proportional to an elevation in the population of both susceptible and vaccinated individuals.

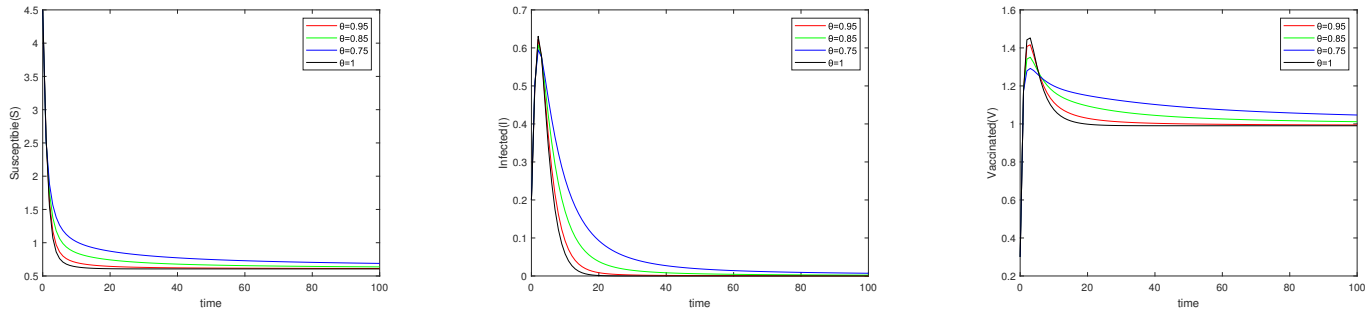

(**a**) (**b**) (**c**)

Figure 2. (**a**–**c**) Effects of θ on S, I, and V when $R_0 < 1$.

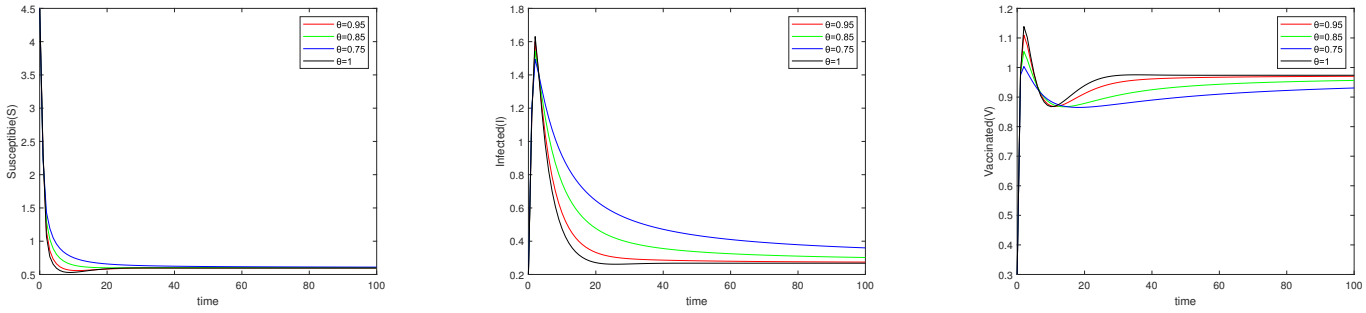

(**a**) (**b**) (**c**)

Figure 3. (**a**–**c**) Effects of θ on S, I, and V when $R_0 > 1$.

Figure 3 confirms that when $\beta = 1.05, d = 0.1, p = 0.15$, which corresponds to $R_0 = 2.9743$, the endemic equilibrium point E_e is locally asymptotically stable. For the infected compartment, especially in the endemic state, as depicted in Figure 3b, a reduction in the value of θ leads to an enhancement in the system's memory capacity, subsequently causing a deceleration in the rate of convergence. This means that it takes longer to eliminate the disease. Figure 4 illustrates the impact of the vaccination ratio q for newborns on the model. Here comes an interesting finding: the change in q significantly affects the variations in S and V. When the vaccination ratio escalates, the quantity of S diminishes, whereas the count of V augments. However, the change in q has a minor effect on I. This is because by analyzing the expression of R_0, we can see that a higher q leads to a lower value of R_0, making the disease more controllable.

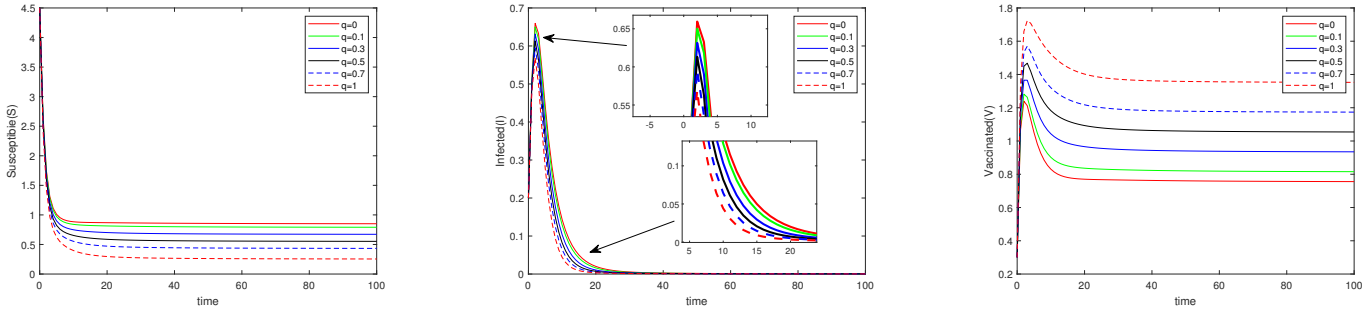

(**a**) (**b**) (**c**)

Figure 4. (**a**–**c**) Effect of q on S, I, and V.

Figure 5 demonstrates the influence of the vaccination ratio p among the susceptible population on the model. Clearly, when the p value decreases, infections accumulate at a gradual pace, eventually contributing to the widespread dissemination of the disease and its evolution into an endemic state. Figure 6 shows the effect of vaccine effectiveness σ on the model. A higher value of σ indicates lower vaccine effectiveness. It can be observed that the level of vaccine effectiveness has a significant impact on both the infected population and the vaccinated population. Higher effectiveness leads to a lower peak of infection, and the disease eventually subsides, along with a reduction in the number of vaccinations, thus saving on vaccination costs.

When considering a model that does not include vaccination, we set the parameters related to vaccination to zero, $p = q = \varepsilon = 0$, and $\sigma = 1$. In this case, the basic reproduction number of the model without vaccination is $R_0^{wv} = \frac{\beta\Lambda}{d(d+\alpha+\gamma)}$. We observe that $R_0 = \frac{\varepsilon+d+\sigma p-(1-\sigma)dq}{d+\varepsilon+p} R_0^{wv}$, thus $R_0 < R_0^{wv}$. This correlation highlights the influence that vaccination has on diminishing the basic reproduction number, making the disease more controllable.

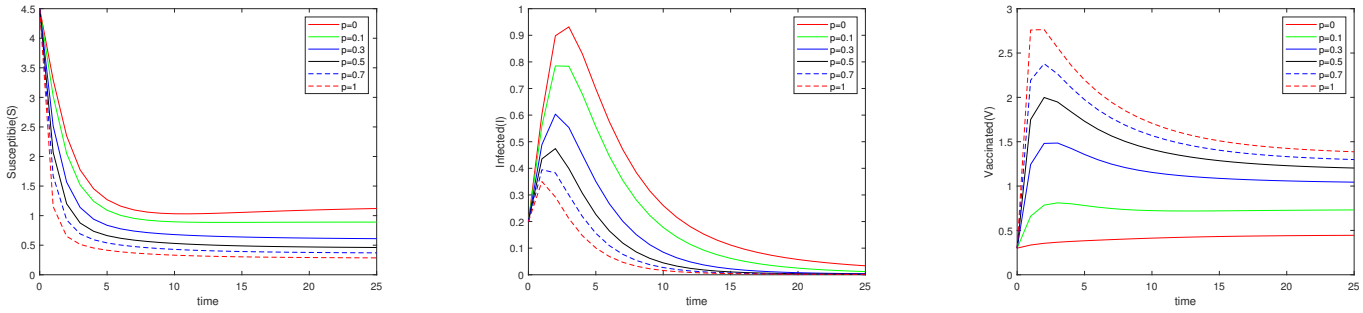

(**a**) (**b**) (**c**)

Figure 5. (**a**–**c**) Effect of p on S, I, and V.

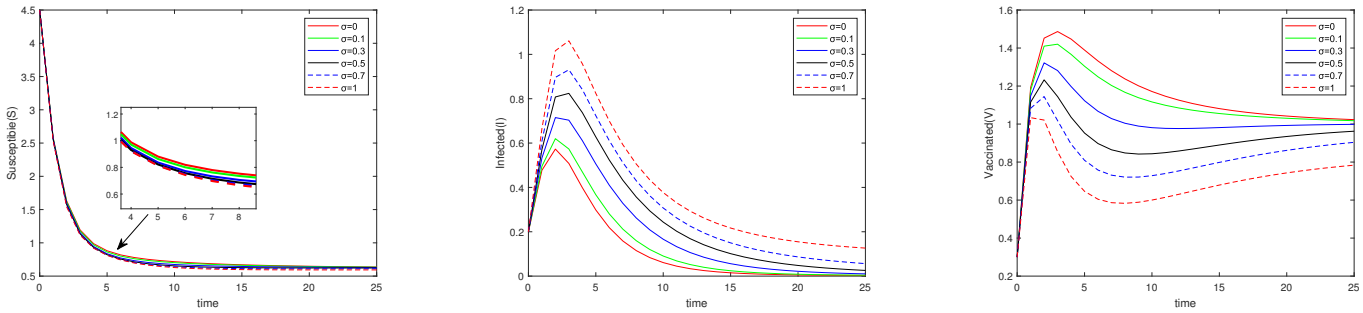

(**a**) (**b**) (**c**)

Figure 6. (**a**–**c**) Effect of σ on S, I, and V.

It should be noted that R_0 is independent of m, so it does not alter the stability at the equilibrium point, which is evident in Figure 7. Although m changes the peak value of I, it does not alter its equilibrium state.

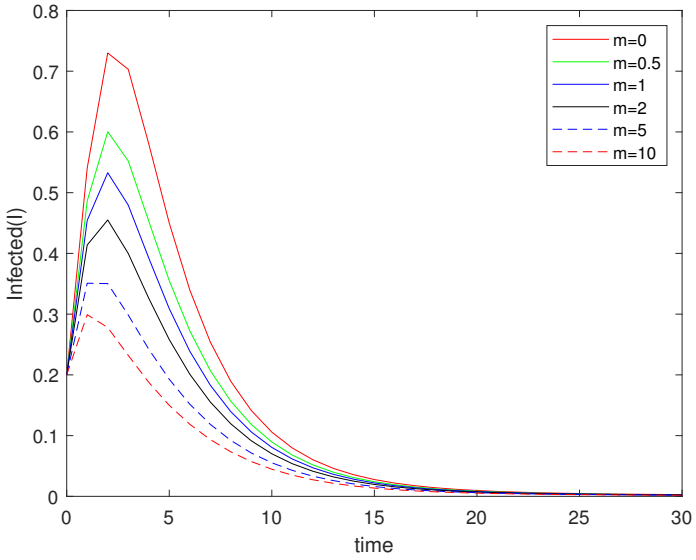

Figure 7. Effect of m on I.

7.2. Numerical Simulation with Control Measures

In this subsection, we introduce the numerical results of the model after the introduction of control measures. To more effectively manage the dissemination of diseases and mitigate the expenses associated with implementing preventive measures, four distinct control strategies were devised to combat the dissemination of the disease:

Strategy A: Using isolation, vaccination, and treatment control (i.e., $u_1, u_2, u_3 \neq 0$).
Strategy B: Using vaccination and treatment control (i.e., $u_2, u_3 \neq 0$ and $u_1 = 0$).
Strategy C: Using isolation and treatment control control (i.e., $u_1, u_3 \neq 0$ and $u_2 = 0$).
Strategy D: Using isolation and vaccination control (i.e., $u_1, u_2 \neq 0$ and $u_3 = 0$).

Figure 8 illustrates the variation in the objective function $J(u)$ in the four strategies. It is evident that strategy A yields the most effective control outcome. Figure 9 depicts the curves of the control variables $u_i, i = 1, 2, 3.$ varying with time under different control strategies. Moreover, as seen in Figure 9a, for control strategy A, control measure u_1 should be implemented on a large scale in the initial days and then stopped after 13 days. Control measure u_2 needs to maintain the control intensity at around 0.213 after the 22nd day, while control measure u_3 should maintain the control intensity at approximately 0.096 after the 37th day. Figure 9b illustrates that when contrasted with control strategy A, although the final control intensities are not significantly different, the peak intensity of control measure u_3 in strategy B lasts for approximately 13 days. As seen in Figure 9c, in comparison to strategy A, the control measures u_1 and u_3 in strategy C have both increased in terms of time and control intensity. Figure 9d indicates that the control measures u_1 and u_2 in strategy D have also increased in terms of duration and the strength of control applied; however, the rise is not as significant as in control strategy C. As a result, the influence of the control measure u_2 surpasses that of u_3 in terms of effectiveness.

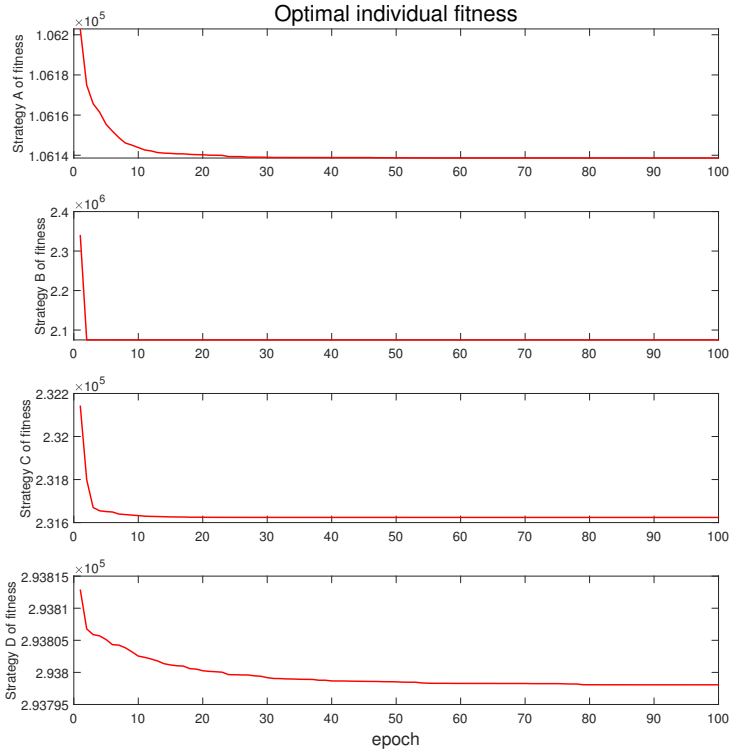

Figure 8. Changes in the objective function under different strategies ($\theta = 0.95$).

Figure 10 illustrates the variations in three variables, S, I, and V, in the model over time when there is no control and when different control strategies are used. Specifically, Figure 10b shows that after the introduction of control measures, the disease will eventually disappear, and when control strategy A is applied, the disease disappears first. Moreover, as the control measure u_3 of strategy C maintains the highest control intensity, Figure 10a reveals that strategy C has the largest susceptible population. Similarly, the control measure u_2 maintains the highest intensity in strategy D, and Figure 10c indicates that when strategy D is used, the vaccinated population reaches the highest level compared to other strategies.

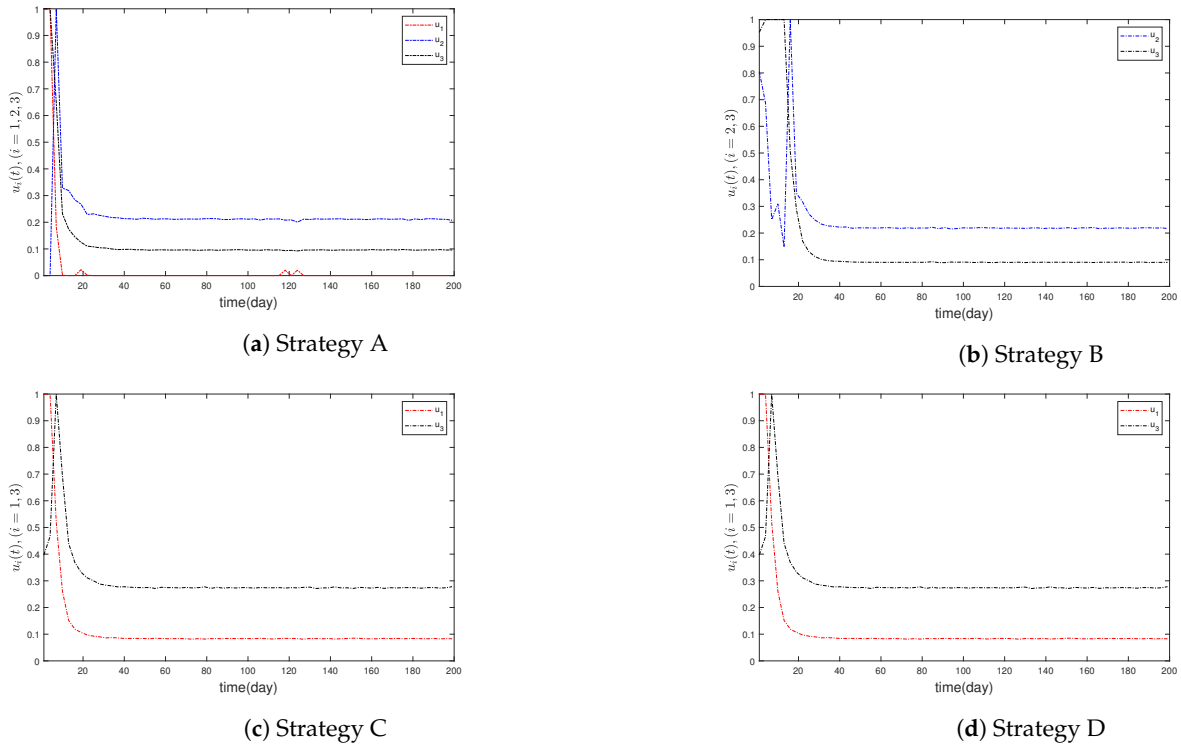

(**a**) Strategy A (**b**) Strategy B

(**c**) Strategy C (**d**) Strategy D

Figure 9. Time series plot of control variables under different strategies.

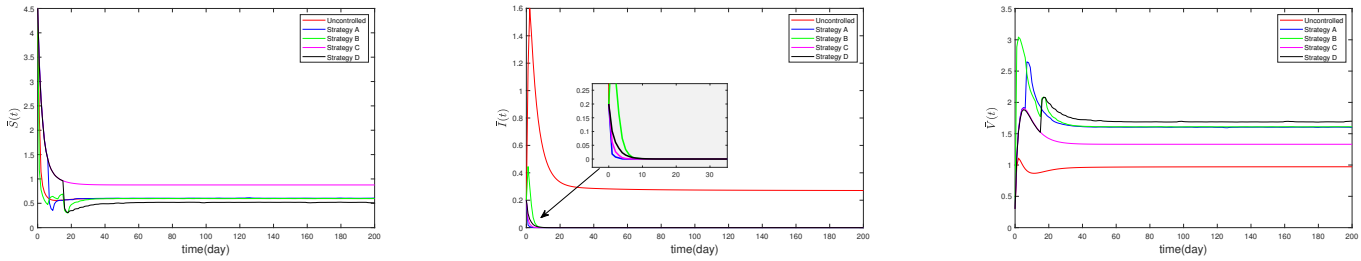

(**a**) (**b**) (**c**)

Figure 10. (**a**–**c**) The impact of different strategies on S, I, and V.

8. Conclusions

In this paper, we propose a fractional-order SIV epidemic model featuring a non-monotonic incidence rate and a continuous vaccination strategy. Initially, to maintain this study's relevance in biology, we examine the model's dynamic characteristics from a fractional-order perspective, which involves verifying the existence and uniqueness of solutions as well as confirming their non-negativity and boundedness.Then, we identify two equilibrium points in the model, namely, the disease-free equilibrium E_0 and the endemic equilibrium E_e, and calculate the basic reproduction number R_0. Furthermore, we investigate the necessary conditions for ensuring the local and global stability of both E_0 and E_e. We demonstrate the critical role of vaccination in disease elimination by investigating its influence on R_0. Additionally, we develop an optimal control strategy to reduce the spread of the disease. In the model, we introduce three control variables, u_1, u_2, and u_3, representing isolation, vaccination, and treatment, respectively. Drawing upon Pontryagin's maximum principle, we formulate the necessary optimality conditions for the fractional-order optimal control problem and introduce particle swarm optimization to enhance the effectiveness of disease control. Finally, the results of numerical simulations indicate that strategy A is superior in terms of curbing the spread of disease.

In future work, our model can take the isolation compartment into consideration, which may be an interesting extension. Bifurcation analysis can also be included in the subsequent model analysis. It is also a good choice to build a model in a stochastic system.

Author Contributions: J.Y.: methodology, software, formal analysis, writing—original draft, and writing—review and editing. W.W.: validation and writing—review and editing. Q.M.: project administration. X.T.: conceptualization, visualization, and writing—review and editing. All authors have read and agreed to the published version of the manuscript.

Funding: This work was supported by the National Natural Science Foundation of China (Nos. 11361104, 12261104), the Youth Talent Program of Xingdian Talent Support Plan (XDYC-QNRC-2022-0514), the Yunnan Provincial Basic Research Program Project (No. 202301AT070016, No. 202401AT070036), and the Science Research Fund of Education Department of Yunnan Province (No. 2024Y468).

Institutional Review Board Statement: Not applicable.

Informed Consent Statement: Not applicable.

Data Availability Statement: Data sharing is not applicable to this article as no data sets were generated or analyzed during the current study.

Conflicts of Interest: The authors declare that there is no conflicts of interest regarding the publication of this paper.

References

1. Khan, T.; Ullah, Z.; Ali, N.; Zaman, G. Modeling and control of the hepatitis B virus spreading using an epidemic model. *Chaos Solitons Fractals* **2019**, *124*, 1–9. [CrossRef]
2. Nill, F. Endemic oscillations for SARS-COV-2 Omicron—A SIRS model analysis. *Chaos Solitons Fractals* **2023**, *173*, 113678. [CrossRef] [PubMed]
3. Girardi, P.; Gaetan, C. An SEIR Model with Time-Varying Coefficients for Analyzing the SARS-CoV-2 Epidemic. *Risk Anal.* **2023**, *43*, 144–155. [CrossRef] [PubMed]
4. Zhang, G.; Li, Z.; Din, A.; Chen, T. Dynamic analysis and optimal control of a stochastic COVID-19 model. *Math. Comput. Simul.* **2024**, *215*, 498–517. [CrossRef]
5. Vargas-De-León, C. On the global stability of SIS, SIR and SIRS epidemic models with standard incidence. *Chaos Solitons Fractals* **2011**, *44*, 1106–1110. [CrossRef]
6. Memon, Z.; Qureshi, S.; Memon, B.R. Assessing the role of quarantine and isolation as control strategies for COVID-19 outbreak: A case study. *Chaos Solitons Fractals* **2021**, *144*, 110655. [CrossRef] [PubMed]
7. Anderson, R.M.; May, R.M. *Infectious Diseases of Humans: Dynamics and Control*; Oxford University Press: Oxford, UK, 1991.
8. Alexander, M.E.; Bowman, C.; Moghadas, S.M.; Summers, R.; Gumel, A.B.; Sahai, B.M. A vaccination model for transmission dynamics of influenza. *SIAM J. Appl. Dyn. Syst.* **2004**, *3*, 503–524. [CrossRef]
9. Elbasha, E.H.; Gumel, A.B. Theoretical assessment of public health impact of imperfect prophylactic HIV-1 vaccines with therapeutic benefits. *Bull. Math. Biol.* **2006**, *68*, 577–614. [CrossRef]
10. Kermack, W.O.; McKendrick, A.G. A contribution to the mathematical theory of epidemics. *Proc. R. Soc. Lond. Ser. A Contain. Pap. Math. Phys. Character* **1927**, *115*, 700–721.
11. Brauer, F.; Van den Driessche, P.; Wu, J.; Allen, L.J. *Mathematical Epidemiology*; Springer: Berlin/Heidelberg, Germany, 2008; Volume 1945.
12. Brauer, F.; Castillo-Chavez, C.; Castillo-Chavez, C. *Mathematical Models in Population Biology and Epidemiology*; Springer: Berlin/Heidelberg, Germany, 2012; Volume 2.
13. Capasso, V.; Serio, G. A generalization of the Kermack-McKendrick deterministic epidemic model. *Math. Biosci.* **1978**, *42*, 43–61. [CrossRef]
14. Liu, W.-m.; Levin, S.A.; Iwasa, Y. Influence of nonlinear incidence rates upon the behavior of SIRS epidemiological models. *J. Math. Biol.* **1986**, *23*, 187–204. [CrossRef] [PubMed]
15. Jang, S.R.J. Backward bifurcation in a discrete SIS model with vaccination. *J. Biol. Syst.* **2008**, *16*, 479–494. [CrossRef]
16. Parsamanesh, M.; Mehrshad, S. Stability of the equilibria in a discrete-time sivs epidemic model with standard incidence. *Filomat* **2019**, *33*, 2393–2408. [CrossRef]
17. Farnoosh, R.; Parsamanesh, M. Disease extinction and persistence in a discrete-time SIS epidemic model with vaccination and varying population size. *Filomat* **2017**, *31*, 4735–4747. [CrossRef]
18. Parsamanesh, M.; Erfanian, M.; Mehrshad, S. Stability and bifurcations in a discrete-time epidemic model with vaccination and vital dynamics. *BMC Bioinform.* **2020**, *21*, 1–15. [CrossRef] [PubMed]

19. Parsamanesh, M.; Erfanian, M. Stability and bifurcations in a discrete-time SIVS model with saturated incidence rate. *Chaos Solitons Fractals* **2021**, *150*, 111178. [CrossRef]
20. Elbaz, I.M.; Sohaly, M.A.; El-Metwally, H. Random dynamics of an SIV epidemic model. *Commun. Nonlinear Sci. Numer. Simul.* **2024**, *131*, 107779. [CrossRef]
21. Baleanu, D.; Sajjadi, S.S.; Asad, J.H.; Jajarmi, A.; Estiri, E. Hyperchaotic behaviors, optimal control, and synchronization of a nonautonomous cardiac conduction system. *Adv. Differ. Equations* **2021**, *2021*, 157. [CrossRef]
22. Jajarmi, A.; Baleanu, D.; Zarghami Vahid, K.; Mobayen, S. A general fractional formulation and tracking control for immunogenic tumor dynamics. *Math. Methods Appl. Sci.* **2022**, *45*, 667–680. [CrossRef]
23. Huo, J.; Zhao, H.; Zhu, L. The effect of vaccines on backward bifurcation in a fractional order HIV model. *Nonlinear Anal. Real World Appl.* **2015**, *26*, 289–305. [CrossRef]
24. Pinto, C.M.; Carvalho, A.R. A latency fractional order model for HIV dynamics. *J. Comput. Appl. Math.* **2017**, *312*, 240–256. [CrossRef]
25. Arqub, O.A.; El-Ajou, A. Solution of the fractional epidemic model by homotopy analysis method. *J. King Saud-Univ.-Sci.* **2013**, *25*, 73–81. [CrossRef]
26. Jana, S.; Mandal, M.; Nandi, S.K.; Kar, T.K. Analysis of a fractional-order SIS epidemic model with saturated treatment. *Int. J. Model. Simul. Sci. Comput.* **2021**, *12*, 2150004. [CrossRef]
27. Podlubny, I. *Fractional Differential Equations*; Academic: San Diego, CA, USA, 1999.
28. Dai, L.; Liu, X.; Chen, Y. Global dynamics of a fractional-order SIS epidemic model with media coverage. *Nonlinear Dyn.* **2023**, *111*, 19513–19526. [CrossRef]
29. Phukan, J.; Dutta, H. Dynamic analysis of a fractional order SIR model with specific functional response and Holling type II treatment rate. *Chaos Solitons Fractals* **2023**, *175*, 114005. [CrossRef]
30. Ameen, I.; Baleanu, D.; Ali, H.M. An efficient algorithm for solving the fractional optimal control of SIRV epidemic model with a combination of vaccination and treatment. *Chaos Solitons Fractals* **2020**, *137*, 109892. [CrossRef]
31. Majee, S.; Jana, S.; Das, D.K.; Kar, T. Global dynamics of a fractional-order HFMD model incorporating optimal treatment and stochastic stability. *Chaos Solitons Fractals* **2022**, *161*, 112291. [CrossRef]
32. Li, Y.; Chen, Y.; Podlubny, I. Stability of fractional-order nonlinear dynamic systems: Lyapunov direct method and generalized Mittag–Leffler stability. *Comput. Math. Appl.* **2010**, *59*, 1810–1821. [CrossRef]
33. Diekmann, O.; Heesterbeek, J.A.P.; Metz, J.A.J. On the definition and the computation of the basic reproduction ratio R 0 in models for infectious diseases in heterogeneous populations. *J. Math. Biol.* **1990**, *28*, 365–382. [CrossRef]
34. Van den Driessche, P.; Watmough, J. Reproduction numbers and sub-threshold endemic equilibria for compartmental models of disease transmission. *Math. Biosci.* **2002**, *180*, 29–48. [CrossRef]
35. Van den Driessche, P.; Watmough, J. Further notes on the basic reproduction number. In *Mathematical Epidemiology*; Springer: Berlin/Heidelberg, Germany, 2008; pp. 159–178.
36. La Salle, J.P. *The Stability of Dynamical Systems*; SIAM: Bangkok, Thailand, 1976.
37. Lyapunov, A.M. The general problem of the stability of motion. *Int. J. Control* **1992**, *55*, 531–534. [CrossRef]
38. Kopp, R.E. Pontryagin maximum principle. In *Mathematics in Science and Engineering*; Elsevier: Amsterdam, The Netherlands, 1962; Volume 5, pp. 255–279.
39. Lukes, D.L. Differential equations: Classical to controlled. *Am. Math. Mon.* **1982**, *92*, 223–225.
40. Diethelm, K. Efficient solution of multi-term fractional differential equations using P (EC) m E methods. *Computing* **2003**, *71*, 305–319. [CrossRef]
41. Kennedy, J.; Eberhart, R. Particle swarm optimization. In Proceedings of the ICNN'95-International Conference on Neural Networks, Perth, WA, Australia, 27 November–1 December 1995; IEEE: Piscataway, NJ, USA, 1995; Volume 4, pp. 1942–1948.